A Load Model to Reduce Computational Effort in Real-Time Simulation of Asymmetrical Short Circuits

Cosimo Iurlaro
DEI - Politecnico di Bari
Bari, Italy
cosimo.iurlaro@poliba.it

Karthik Rajashekaraiah
ITEP - Karlsruhe Institute of Technology
Karlsruhe, Germany
karthik.rajashekaraiah@kit.edu

Giovanni De Carne
ITEP - Karlsruhe Institute of Technology
Karlsruhe, Germany
giovanni.carne@kit.edu

Sergio Bruno
DEI - Politecnico di Bari
Bari, Italy
sergio.bruno@poliba.it

2025 IEEE Kiel PowerTech | 979-8-3315-4397-6/25/$31.00 ©2025 IEEE | DOI: 10.1109/PowerTech59965.2025.11180542

***Abstract*—Transient analyses of electrical networks demand highly accurate models to represent component behavior precisely, thereby increasing the computational burden of simulations. This aspect becomes critical when conducting real-time simulations, such as Hardware-in-the-Loop, as the computational weight of the models can make some case studies unfeasible and require increasingly powerful devices, significantly raising the cost of real-time test systems. This paper proposes a low computational cost approach to model single-phase dynamic resources for stationary and dynamic power system analyses. The strategy is based on the instantaneous p-q theory and avoids heavy blocks/calculations such as Root-Mean-Square, Phase-Locked-Loop, and abc-$dq0$ coordinate transformations. Moreover, a Single-Phase P-Q Theory-based Dynamic Load model is introduced and validated on Matlab/Simulink platform under severe transient network conditions, namely LG and LL asymmetrical short circuits. The model is compared with static and dynamic load models of the simulation platform.**

***Index Terms*—Instantaneous p-q theory, dynamic load modeling, single-phase load model, real-time simulation, asymmetrical faults, low computational burden.**

I. Introduction

The use of real-time simulation systems has become widespread in research and industry for several applications [1], [2]. By connecting real-time simulators to various components it is possible to test real components and systems under the most diverse operating conditions. This significantly accelerates their development and reduces the time from their conception to implementation and market release [3], [4]. In most power system applications, this technology is employed to connect physical devices to electrical network models simulated in real-time [4].

Hardware-in-the-Loop and Power Hardware-in-the-Loop simulations enable testing of electrical devices under various adverse grid conditions, validating them and their control systems [5], [6]. In such tests, the components of the simulated networks (loads, generators, transformers, etc.) must be represented in detail to capture their behavior during electrical transients [7]. These models, however, come with a high computational cost, which increases as the required precision and the number of connected components (including their control systems) grow. This, in turn, results in higher computational power demands for executing the tests and increased costs for real-time simulators [8].

With regard to load modeling, computational cost can be easily contained by adopting static RLC models to represent an aggregation of loads at system buses [9]. However, these models can only be applied if this aggregation behaves as a constant impedance load. In most cases, though, the aggregation includes various types of loads, such as constant power loads or dynamic loads whose response to voltage and frequency variations might vary according to their nature. In addition, loads can also have a dynamic behavior due to automatic control actions which could be applied according to the operating conditions (e.g., demand response actions). Clearly, these dynamics can be represented only through an appropriate dynamic load modeling. However, dynamic load models commonly adopted in simulation software are computationally much heavier than the static ones, as they involve blocks and calculations such as synchronization via Phase-Locked Loop (PLL), abc-$dq0$ coordinate transformations, Root Mean Square (RMS) value computation, and similar operations.

Exploiting the instantaneous p-q theory introduced in [10], the authors of [11] proposed a computationally efficient method for modeling dynamic electrical loads/sources in Matlab/Simulink. The authors demonstrated that this approach allows the exploitation of the same advantages given by using dynamic electrical load models based on conventional approaches (e.g., PLL, RMS, and abc-$dq0$ transformation) with significantly reduced computational costs and without affecting the accuracy of the results. Being based on instantaneous power values in the time domain within $\alpha\beta0$ coordinates, this model is suitable for both static and dynamic analyses of balanced three-phase systems. Robustness and accuracy of the model were also analyzed and validated under extreme network conditions, such as short circuits, by the authors in [12]. In addition, the model was used in Power Hardware-in-the-Loop tests to reduce the computational effort necessary to emulate the behavior of a real distribution grid [6]. However, it should be stressed out that the model presented in [11], [12] relies on the Clarke transformation to compute the $\alpha\beta0$ components from the three-phase voltages

abc, and can only be adopted to model balanced three-phase loads.

In this paper, these limitations are overcome developing a Single-Phase P-Q Theory-based Dynamic Load Model. The proposed model utilizes a Second-Order Generalized Integrator Frequency-Locked Loop (SOGI-FLL) [13] to generate voltage references in the $\alpha\beta0$ coordinate reference system and synchronize the model with the network. Unlike [12], where only symmetrical short circuits could be applied, in this paper, the proposed model is tested under asymmetrical short circuit conditions. In addition, by combining single-phase units, the model can also be employed to emulate unbalanced three-phase loads, in both balanced or unbalanced conditions.

The paper is structured as follows: Section II introduces the p-q theory and the proposed load model. Section III describes the network model used for testing and the load models compared in this study. In Section IV, the behavior of the proposed load model is analyzed and compared during asymmetrical short circuits in the network. Section V highlights the computational advantages of the proposed model. Finally, the conclusion section closes the discussion.

II. P-Q THEORY-BASED DYNAMIC LOAD MODELING

In real-time simulations, the behavior of a dynamic load connected to a power grid model is typically simulated via a controlled current source that follows a specific current reference (as in Fig. 1). This reference is generated in order to replicate the active and reactive power absorbed by the load. To achieve this, measurements of voltage amplitude and angle are required in order to determine the amplitude and angle deviation of the current. Typically, voltage angle and amplitude are calculated using a Phase-Locked Loop (PLL) and the computations are performed in $dq0$-coordinates. As already mentioned, the proposed dynamic load model avoids the use of these high computational cost calculations and generates the current reference using a SOGI-FFL and instantaneous p-q theory.

A. Instantaneous P-Q theory approach

This section describes the mathematical approach of the p-q theory, introduced by [10]. To improve the readability of the mathematical formulation, the time dependence of electrical variables, such as voltage and current, is omitted. The v_α and v_β components, obtained in [11], [12] from the three-phase voltage waveforms via the Clarke transform, in this single-phase model, are obtained using a Second-Order Generalized Integrator Frequency-Locked Loop (SOGI-FLL). The operation and implementation of the SOGI-FLL are described in detail in [13]. As indicated by several papers [14], [15], the SOGI-FLL is well-known and widely used in literature for its accuracy and simplicity.

$$\begin{aligned} v_{\alpha\beta} &= v_\alpha + \jmath v_\beta \\ i_{\alpha\beta} &= i_\alpha + \jmath i_\beta \end{aligned} \tag{1}$$

The instantaneous complex power s can be calculated as the product of the voltage $v_{\alpha\beta}$ and the conjugate of the current $i^*_{\alpha\beta}$ in $\alpha\beta$ coordinates, from which the instantaneous active and reactive powers can be derived as in eq. (2). Considering instantaneous values of voltage and current for the calculation of the complex power, s represents the exact instantaneous complex power at each moment, both in steady-state and transient conditions.

$$s = v_{\alpha\beta} \cdot i^*_{\alpha\beta} = (v_\alpha i_\alpha + v_\beta i_\beta) + \jmath(v_\beta i_\alpha - v_\alpha i_\beta) = p + \jmath q \tag{2}$$

From the expressions of active and reactive power in (2), the expressions of current in $\alpha\beta$ coordinates (3) can be derived.

$$\begin{aligned} i_\alpha &= \frac{v_\alpha}{v_\alpha^2 + v_\beta^2} p + \frac{v_\beta}{v_\alpha^2 + v_\beta^2} q \\ i_\beta &= \frac{v_\beta}{v_\alpha^2 + v_\beta^2} p + \frac{-v_\alpha}{v_\alpha^2 + v_\beta^2} q \end{aligned} \tag{3}$$

The current i_α represents the actual current exchanged by the single-phase resource and can be used as the current reference for a single-phase current source model. On the other hand, i_β simply represents the quadrature component of i_α useful for calculation purposes. This current becomes significant when dealing with a three-phase energy resource, such as an unbalanced electrical load. The currents flowing in the three phases can be obtained through the inverse Clarke transformation.

B. Single-Phase P-Q Theory-based Dynamic Load Model

To visually represent the p-q theory just introduced, a single-phase dynamic load model based on the p-q theory was developed using MATLAB/Simulink. This model, referred to as PQL (P-Q Theory-based Dynamic Load), is designed to be computationally efficient while incorporating all the advanced functionalities of a dynamic load model.

To demonstrate the actual computational advantages of the proposed model, the load behavior considered was that of an exponential load model, the same load behavior adopted by the Simulink "Three-Phase Dynamic Load" model. The proposed PQL model, in fact, will be compared with a single-phase version of that model, referred to as SDL (Simulink Dynamic Load) and available on the software's official website [16].

The structure of the model is shown in Fig. 1. The measured voltage waveform is decomposed into its $\alpha\beta$ components using a SOGI-FLL ($v_{\alpha\beta}$). The active and reactive power references (p_{ref} and q_{ref}) are compared with p_m and q_m, which represent the active and reactive power calculated from voltage and current measurements using eq. (2). The error is sent to a PI controller, which generates the reference active and reactive power values for the p-q theory block. In this block, using eq. (3), the current in $\alpha\beta$ coordinates is calculated. While both components of the current are used for calculating the measured power, only the component along

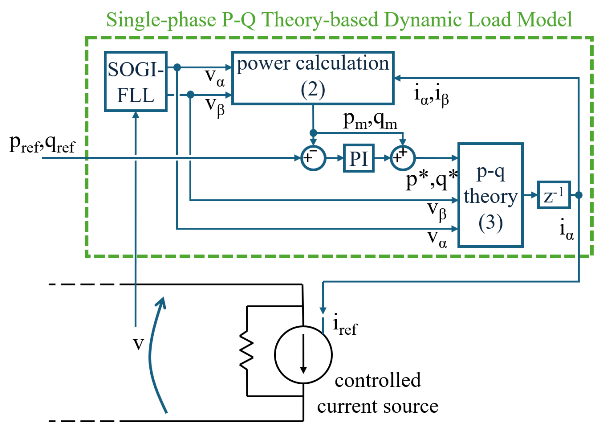

Fig. 1. Schematic of the proposed single-phase p-q theory-based dynamic load

the α axis is useful as current reference for the controlled current source.

Please note that the proposed model can also be used to track dynamically the active and reactive power set-points p_{ref} and q_{ref}, and represent the behavior of any kind of controlled energy resource (for example demand response, batteries, generators, etc.).

III. Test case description

To demonstrate the proper functioning of the proposed single-phase load model and its computation advantages for real-time simulations, a real-time model of the IEEE 123-node distribution feeder network was adopted. The IEEE 123-node test feeder operates at a nominal voltage of 4.16 kV and 60 Hz. This network supplies both balanced and unbalanced loads scattered throughout the system and is characterized by a combination of overhead and underground lines. Moreover, the network includes multiple single-phase voltage regulators, shunt capacitor banks, and switches. The network scheme is shown in Fig. 2.

The tests were conducted by comparing the response of three grid models, each representing the same network in Fig. 2, but built adopting a different load model. The models were implemented on a Simulink-based platform, whereas real-time simulations were executed with a time-step of T_s = 50μs on an OP5700 real-time digital simulator by OPAL-RT. The reference model was available in the RT-Lab software library of OPAL-RT, whose accuracy has been extensively demonstrated by the authors in [17]. The three different load models used to build the network are listed below.

- Simulink Static Load (SSL): the load model used by the reference grid model. The behavior of the load is described by a single differential equation of the series RLC circuit. Thanks to its accuracy and low computational effort, the results obtained using this load model are considered as a benchmark for the analysis in this work.
- Simulink Dynamic Load (SDL): the single-phase version of the "Three-Phase Dynamic Load" present in Simulink. Differently from the SSL model, it is characterized by several blocks and functions that make it fully controllable. For the purpose of comparison, the dynamic model was set to reproduce the behavior of a constant-impedance load (i.e. in the exponential model, the exponents are equal 2).
- P-Q Theory-based Dynamic Load (PQL): the proposed dynamic load model. It includes all the functions of the SDL model but with a lower computational cost.

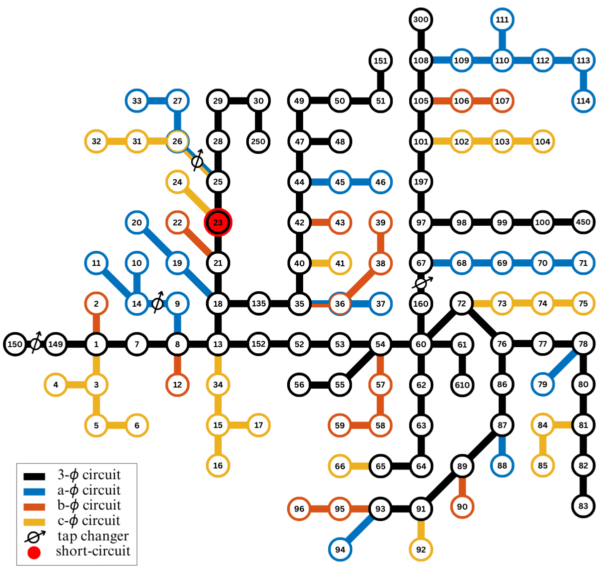

Fig. 2. Scheme of the IEEE 123-node distribution feeder

The three networks were built by simply replacing the SSL load models from the reference model in [17] with the SDL and PQL models. Three-phase loads were implemented using star or delta connections of three single-phase load models. Differently from the SSL model, the SDL and PQL models are characterized by several blocks and functions that make them fully controllable. Anyway, in order to compare the models, the SDL and PQL models are controlled as constant impedance loads. The network model with SSL loads is considered the benchmark for the analysis since its behavior is governed by the differential equation of a physical series RLC circuit. This allows it to more accurately represent the behavior of a constant impedance load compared to the other two models, which approximate load behavior using a mathematical load model.

IV. Short-circuit analysis

This section compares the behavior of the SDL and PQL models with the SSL model during transients caused by asymmetric faults in the network. Two types of faults are presented in this work: an LG fault occurring on phase-a and an LL fault occurring between phase-b and phase-c. Bus#23 was selected as the location for introducing a fault and analyzing the network's response. The network behavior was analyzed over a 1-second simulation period, during which a fault occurs at 0.5 seconds and persists for 3 cycles (0.05 seconds). In order to compare the errors made using the two models (SDL and PQL) compared to the reference model (SSL), the mean and maximum absolute percentage errors, related to the instantaneous RMS reference value, have been calculated during all the transient (from 0.5 to 0.6 seconds). These results are shown in Tables I and II and discussed in the following subsections. The relative errors reach high percentages because the voltage and current experience very low values and significant fluctuations during the fault. In these cases, almost negligible errors can provide high relative errors. For this reason, these errors can be only considered in order to compare the two models (SDL and PQL) and not as indexes of model quality.

A. LG fault analysis

In Fig. 3 and Fig. 4, the voltage and current waveforms on the three phases of the bus#23 are shown. The voltage and current behavior differences between the three network models are hard to appreciate. Some insets are displayed in order to better appreciate the differences. The voltage amplitude drops from 0.9142 to 0.07062 p.u. on the faulted phase, while the current amplitude rises from 0.07178 to 4.512 p.u..

Focusing attention on the faulted phase-a during the transient, as is possible to read on Tables I and II, the SDL model resulted in a lower MAPE compared to the PQL model. Conversely, the maximum error was lower when using the PQL model. As a result, the PQL model presented voltage and current waveforms that were slightly more different from

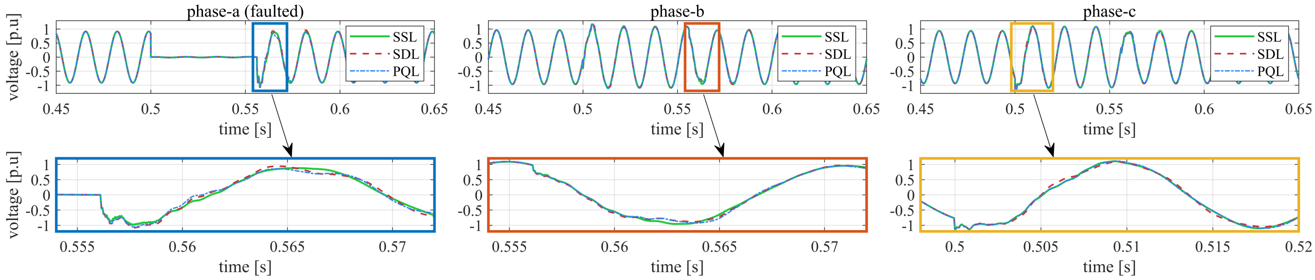

Fig. 3. Voltage waveforms during LG fault test at bus#23, shown for each phase and load model.

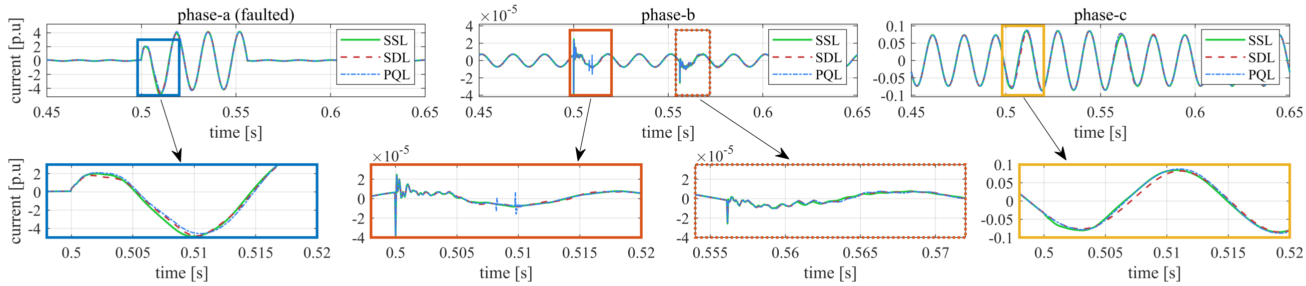

Fig. 4. Current waveforms during LG fault test at bus#23, shown for each phase and load model.

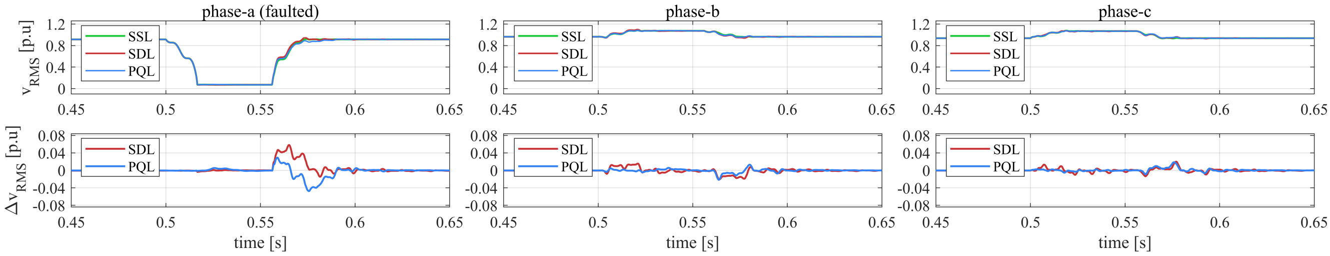

Fig. 5. RMS voltages and their deviations from the SSL model during LG fault test at bus#23, shown for each phase and load model.

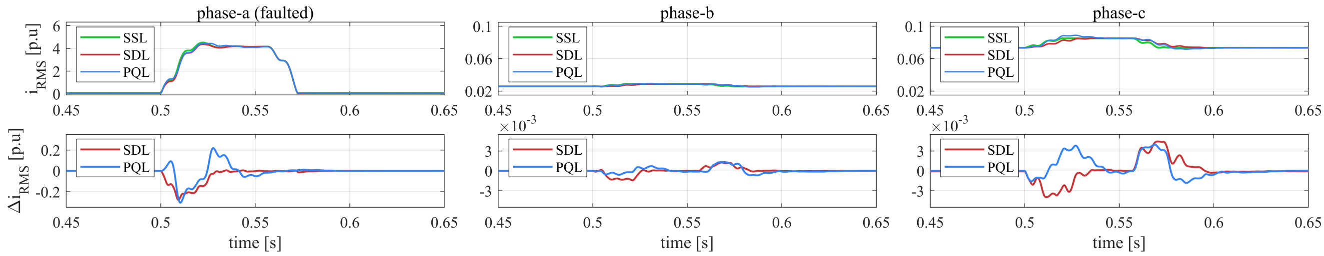

Fig. 6. RMS currents and their deviations from the SSL model during the LG fault test at bus#23, shown for each phase and load model.

TABLE I
MEAN ABSOLUTE PERCENTAGE ERROR (MAPE) OF VOLTAGE AND CURRENT TRAJECTORIES [%].

		v	v_{rms}	i	i_{rms}
LG fault phase-a	SDL	2.9877	1.6661	2.8231	2.9198
	PQL	3.3219	1.8086	4.3512	3.5834
LL fault phase-b	SDL	4.0890	0.7524	3.9627	1.9700
	PQL	4.0340	1.2595	3.7751	1.3583
LL fault phase-b	SDL	4.5567	1.7909	1.9847	1.8859
	PQL	4.3363	1.3698	1.6600	1.6010

TABLE II
MAXIMUM ABSOLUTE PERCENTAGE ERROR OF VOLTAGE AND CURRENT TRAJECTORIES [%].

		v	v_{rms}	i	i_{rms}
LG fault phase-a	SDL	49.6082	9.3381	33.9237	21.3870
	PQL	40.7606	6.2398	39.7201	14.4714
LL fault phase-b	SDL	31.7610	4.7267	36.0589	8.8729
	PQL	23.2986	7.3337	33.0041	8.1706
LL fault phase-b	SDL	29.3768	10.1077	25.4137	12.2968
	PQL	26.6647	7.6835	20.2388	10.7422

the reference waveforms compared to the SDL model, but it avoided extreme deviations from the reference behaviors. These behaviors also reflect on the mean and maximum deviations collected on the RMS trajectories.

The RMS voltage and current behaviors, along with their deviations from the reference behaviors using the SSL model, are shown in Fig. 5 and Fig. 6. Granted that both SDL and PQL models demonstrated high accuracy, the proposed PQL model exhibited slightly better performance.

B. LL fault analysis

Also in this test, both the SDL and PQL models demonstrated high accuracy. In Fig. 7, the voltage waveforms of the three phases at bus#23 are shown, including some enlargements. Although the voltage waveform on phase-b

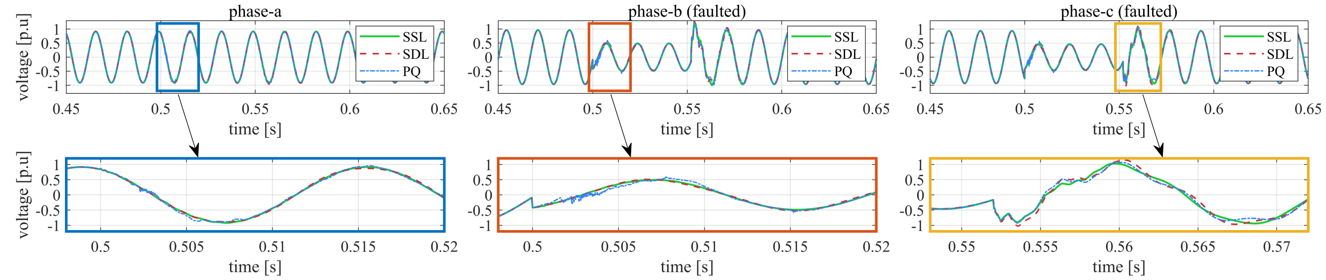

Fig. 7. Voltage waveforms during LL fault test at bus#23, shown for each phase and load model.

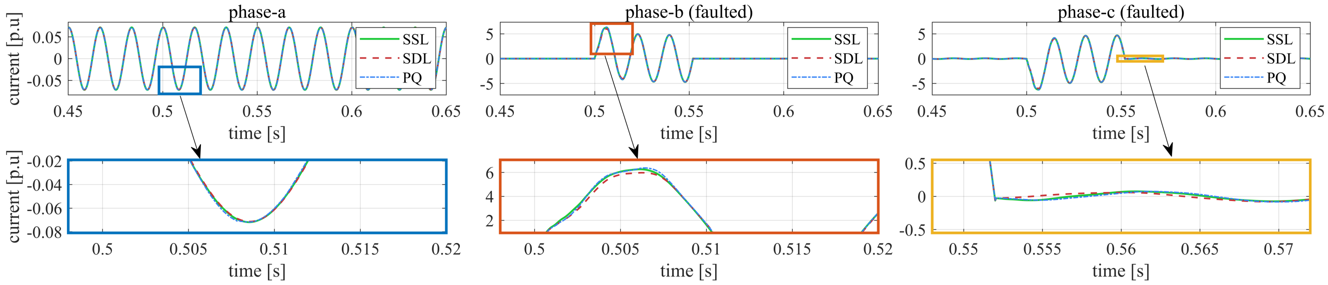

Fig. 8. Current waveforms during LL fault test at bus#23, shown for each phase and load model.

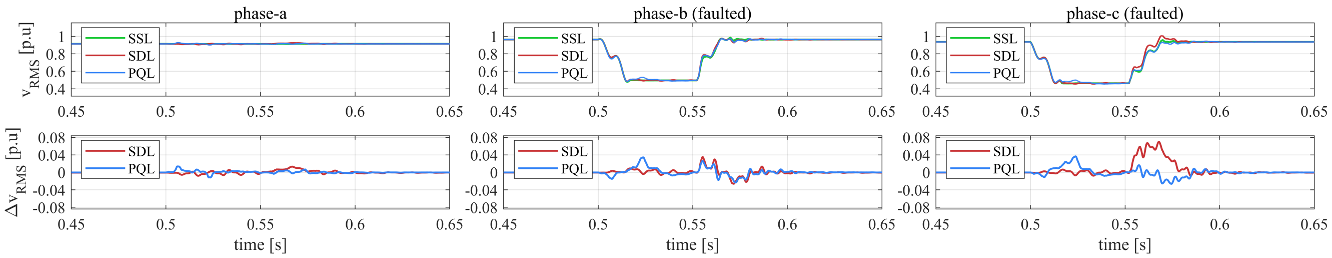

Fig. 9. RMS voltages and their deviations from the SSL model during LL fault test at bus#23, shown for each phase and load model.

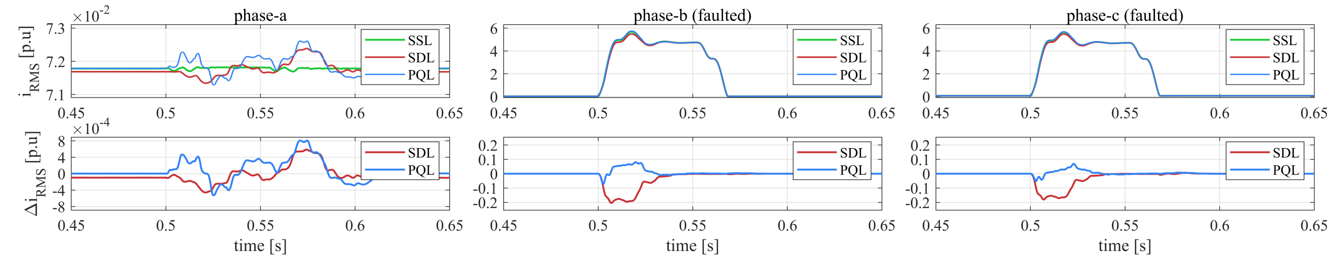

Fig. 10. RMS currents and their deviations from the SSL model during LL fault test at bus#23, shown for each phase and load model.

with the PQL model shows slight noise, which is irrelevant given the small size, it represents the model that most closely follows the trend of the reference SSL model. The differences in the current waveforms are almost imperceptible, even less noticeable than in the case of the LG fault. In this case, due to the two-phase fault, the current in phase-a remained unchanged, while the currents in phases-b and -c, equal in magnitude but opposite in the phase, reached 6.245 per unit during the short circuit.

As was done for the previous test, the RMS voltage and current behaviors and their deviations compared to the reference network behavior using the SSL model were shown (Fig. 9 and Fig. 10). During the transient, the deviations in terms of voltage and current waveforms and RMS values compared to the SSL model are similar for both faulted phases. Between the SDL and PQL models, the latter exhibited a lower deviation from the reference trend in both waveform and RMS value trends. This is further highlighted by the mean and maximum absolute percentage errors presented in Tables I and II. The mean and maximum deviations obtained using the PQL model were consistently lower than those of the SDL model (except for the RMS voltage on phase-b), demonstrating superior accuracy.

V. Computational Burden Analysis

The test results previously discussed demonstrated that the accuracy of proposed PQL model is comparable to the one of the commonly adopted SDL model. However, the PQL model's true value is revealed in its enhanced computational performances, which lead to faster processing times.

The computation time necessary to run the real-time simulation on one single core is shown in Table III for all three load models. It can be noticed that the time required to simulate the proposed PQL dynamic model is very close to the SSL static model. The widely adopted SDL dynamic model is characterized instead by very high computing times.

TABLE III
COMPARISON OF THE COMPUTATIONAL PERFORMANCES OF THE THREE LOAD MODELS

Load Model	Necessary computing time on a single core (μs)	Number of cores needed for a 50μs time-step simulation
SSL	≈59	2
SDL	≈215	5
PQL	≈65	2

Clearly in all cases, if the network models were to be run in real-time adopting a simulation time-step of $50\mu s$, more than one core must be employed to avoid overruns. However, as shown in Table III, PQL and SSL-based models would require the use of only 2 cores. A real-time simulation using the SDL model would require, instead, the use of 5 cores.

The significant advantage of the PQL model is its ability to provide the benefits of dynamic load modeling with the computational speed of static load simulations. In addition, the adoption of the proposed PQL model will allow to solve more complex model without the need of activating more cores. Typically, the enabling of more parallel cores in real-time simulators is subjected to high activation costs, which can be spared thanks to the proposed model.

VI. CONCLUSION

In this work, a lightweight dynamic load modeling approach based on instantaneous p-q theory was proposed to be employed in real-time simulations of asymmetric faults, and a model was developed and tested using the MATLAB/Simulink platform. To demonstrate the proper functioning of the proposed model and its computation advantages for real-time simulations, tests have been conducted on a large unbalanced network model (the IEEE 123-node distribution feeder network).

Compared to the dynamic model provided by Simulink, the proposed model demonstrated higher accuracy in both steady-state and transient operating conditions. Moreover, the proposed model proved to be significantly more computationally efficient then the Simulink dynamic load model, offering the advantage of a dynamic load functionality at a computational cost comparable to that of a purely static load.

Future work will focus on analyzing and testing the model functionalities for constant power and constant current loads. Additionally, the proposed model could be utilized as a controlled current source for network decoupling and for performing PHIL tests on realistic case studies.

REFERENCES

[1] L. F. Gaitán Cubides, J. W. González Sánchez, and L. A. Giraldo Velazquez, "A review of real time digital simulations: Theory and applications for the energy transition," *IEEE Latin America Transactions*, vol. 20, no. 10, pp. 2295–2307, 2022.

[2] S. Bruno, G. Giannoccaro, M. Muzammal Islam, C. Iurlaro, M. La Scala, M. Menga, and C. Rodio, "Control and power hardware-in-the-loop tests for low-inertia power systems," in *2022 AEIT International Annual Conference (AEIT)*, 2022, pp. 1–6.

[3] X. Guillaud, M. O. Faruque, A. Teninge, A. H. Hariri, L. Vanfretti, M. Paolone, V. Dinavahi, P. Mitra, G. Lauss, C. Dufour, P. Forsyth, A. K. Srivastava, K. Strunz, T. Strasser, and A. Davoudi, "Applications of real-time simulation technologies in power and energy systems," *IEEE Power and Energy Technology Systems Journal*, vol. 2, no. 3, pp. 103–115, 2015.

[4] A. Benigni, T. Strasser, G. De Carne, M. Liserre, M. Cupelli, and A. Monti, "Real-time simulation-based testing of modern energy systems: A review and discussion," *IEEE Industrial Electronics Magazine*, vol. 14, no. 2, pp. 28–39, 2020.

[5] Z. Shen, F. Arraño-Vargas, H. R. Wickramasinghe, and G. Konstantinou, "Distributed real-time simulations of power systems: A review," in *2022 IEEE PES 14th Asia-Pacific Power and Energy Engineering Conference (APPEEC)*, 2022, pp. 1–6.

[6] G. Sciumè, C. Iurlaro, S. Bruno, R. Musca, P. Gallo, G. Zizzo, E. R. Sanseverino, and M. L. Scala, "A blockchain-based architecture for tracking and remunerating fast frequency response," *Sustainable Energy, Grids and Networks*, vol. 40, p. 101530, 2024. [Online]. Available: https://www.sciencedirect.com/science/article/pii/S2352467724002595

[7] G. De Carne, G. Lauss, M. H. Syed, A. Monti, A. Benigni, S. Karrari, P. Kotsampopoulos, and M. O. Faruque, "On modeling depths of power electronic circuits for real-time simulation – a comparative analysis for power systems," *IEEE Open Access Journal of Power and Energy*, vol. 9, pp. 76–87, 2022.

[8] M. D. Omar Faruque, T. Strasser, G. Lauss, V. Jalili-Marandi, P. Forsyth, C. Dufour, V. Dinavahi, A. Monti, P. Kotsampopoulos, J. A. Martinez, K. Strunz, M. Saeedifard, X. Wang, D. Shearer, and M. Paolone, "Real-time simulation technologies for power systems design, testing, and analysis," *IEEE Power and Energy Technology Systems Journal*, vol. 2, no. 2, pp. 63–73, 2015.

[9] S. Bruno, C. Iurlaro, M. L. Scala, M. Menga, and M. Semeraro, "A dynamic model of the favignana island non-synchronous power system for power hardware-in-the-loop tests," in *2022 Workshop on Blockchain for Renewables Integration (BLORIN)*, 2022, pp. 107–112.

[10] H. Akagi, E. H. Watanabe, and M. Aredes, *Instantaneous power theory and applications to power conditioning*. John Wiley & Sons, 2017.

[11] K. Rajashekaraiah, C. Iurlaro, S. Bruno, and G. De Carne, "Modelling of 3-phase p-q theory-based dynamic load for real-time simulation," *IEEE Open Access Journal of Power and Energy*, vol. 10, pp. 654–664, 2023.

[12] K. Rajashekaraiah, G. De Carne, C. Iurlaro, M. Semeraro, and S. Bruno, "P-q theory-based dynamic load modelling in short-circuit analysis," in *2023 8th IEEE Workshop on the Electronic Grid (eGRID)*, 2023, pp. 1–5.

[13] P. Rodríguez, A. Luna, R. S. Muñoz-Aguilar, I. Etxeberria-Otadui, R. Teodorescu, and F. Blaabjerg, "A stationary reference frame grid synchronization system for three-phase grid-connected power converters under adverse grid conditions," *IEEE Transactions on Power Electronics*, vol. 27, no. 1, pp. 99–112, 2012.

[14] A. Bamigbade and V. Khadkikar, "Frequency estimators for sogi fll: Modeling, design, and equivalence for fll advancements," *IEEE Trans. Instrum. Meas.*, vol. 71, pp. 1–12, 2022.

[15] S. Golestan, J. M. Guerrero, F. Musavi, and J. C. Vasquez, "Single-phase frequency-locked loops: A comprehensive review," *IEEE Transactions on Power Electronics*, vol. 34, no. 12, pp. 11 791–11 812, 2019.

[16] "Single Phase Dynamic Load Block," https://it.mathworks.com /help/sps/ug/single-phase-dynamic-load-block.html, accessed: 2025-01-16.

[17] B. Ahmed, A. Abdelgadir, N. A. Saied, and A. A. Karrar, "A compensated distributed-parameter line decoupling approach for real time applications," *IEEE Transactions on Smart Grid*, vol. 12, no. 2, pp. 1761–1771, 2020.